

**SEARCHES FOR RARE AND FORBIDDEN DECAYS OF  
CHARM: RECENT RESULTS FROM FNAL**

A. J. Schwartz  
*University of Cincinnati, Cincinnati, Ohio 45221 USA*

ABSTRACT

We review results on rare and forbidden decays of  $D^0$ ,  $D^+$ , and  $D_s^+$  mesons from experiments at FNAL. The decay modes studied have two leptons in the final state and, if observed, would constitute evidence for flavor-changing neutral-current, lepton-flavor-violating, or lepton-number-violating processes. To date, no evidence for these decays has been observed and upper limits are obtained for their branching fractions. These limits can constrain various extensions to the Standard Model. We present new upper limits from FNAL E791 on the branching fractions for more than two dozen three- and four-body decay modes.

**1 Introduction**

Searches for rare and forbidden decays of charm are concerned with final states containing two charged leptons. Such processes occur via flavor-changing

neutral-current amplitudes, lepton-flavor-violating amplitudes (leptons belonging to different families), or lepton-number-violating amplitudes (leptons belonging to one family but having the same sign charge). Diagrams for these amplitudes typically contain new types of particles having high masses; thus, these decays probe energy scales which cannot be accessed directly. For example, the amplitude for the flavor-changing neutral-current decay  $D^+ \rightarrow \pi^+ \mu^+ \mu^-$  is expected to be proportional to  $\tilde{g}^2/M_X^2 \times (\text{phase space})$ , where  $\tilde{g}$  is a coupling constant and  $M_X$  is the mass of some unknown propagator (see Fig. 1). The amplitude for the Standard Model decay  $D^+ \rightarrow \bar{K}^0 \mu^+ \nu$  is proportional to  $g^2/M_W^2 \times (\text{phase space})$ , and thus  $\Gamma(\pi^+ \mu^+ \mu^-)/\Gamma(\bar{K}^0 \mu^+ \nu) = \tilde{g}^4 M_W^4/(g^4 M_X^4) \times (\text{phase space ratio})$ . If  $\tilde{g} \approx g$ , then

$$M_X \approx M_W \left[ \frac{B(D^+ \rightarrow \bar{K}^0 \mu^+ \nu)}{B(D^+ \rightarrow \pi^+ \mu^+ \mu^-)} \times (\text{phase space ratio}) \right]^{1/4}. \quad (1)$$

Inserting numbers one finds that a branching fraction  $B(D^0 \rightarrow \pi^+ \mu^+ \mu^-) \approx 10^{-5}$  corresponds to a mass  $M_X \approx 700 \text{ GeV}/c^2$ .

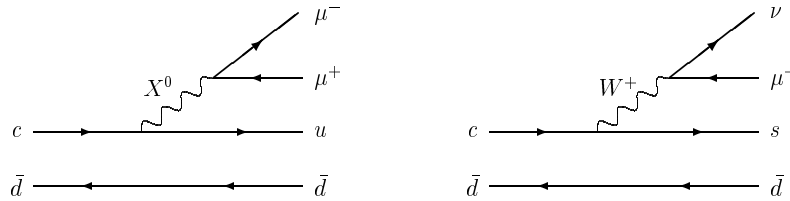


Figure 1: *Nonstandard flavor-changing neutral-current decay (left) and Standard Model charged-current decay (right).*

Over the past year, FNAL E791 has published new limits on branching fractions for 24 different two- and three-body decay modes<sup>1)</sup>, and submitted for publication new limits for 27 additional three- and four-body decay modes<sup>2)</sup>. In most cases the E791 limits are the most stringent available. Here we review these results and also briefly discuss competitive results from other FNAL experiments.

## 2 The E791 Experiment

FNAL E791<sup>1</sup> is a hadroproduction experiment studying the weak decays of charm mesons and baryons. The charm particles were produced by impinging a 500 GeV/c  $\pi^-$  beam on five thin target foils. The most upstream foil consisted of platinum; the other foils consisted of carbon (diamond). All foils were separated by about 15 mm such that  $D$  mesons decayed predominately in the air gaps between foils. The experimental apparatus<sup>3)</sup> consisted of a silicon vertex detector followed by a two-magnet spectrometer, two segmented Cerenkov counters for hadron identification, an electromagnetic calorimeter for electron identification, and iron shielding followed by scintillator counters for muon identification. The downstream silicon vertex detector consisted of 17 planes of silicon and was used to reconstruct decay vertices downstream of the interaction vertex. The spectrometer consisted of 35 planes of drift chambers and two proportional wire chambers. The two dipole magnets bent particles in the horizontal plane and had  $p_T$  kicks of +210 GeV/c and +320 GeV/c. The Cerenkov counters contained gases with different indices of refraction; together they provided  $\pi/K/p$  discrimination over the momentum range 6–60 GeV/c. Data were recorded using a loose transverse energy trigger. After reconstruction, events with evidence of well-separated interaction and decay vertices were retained for further analysis. The experiment took data from September, 1991 to January 1992, recording the world's largest sample of charm decays at that time. The final number of reconstructed decays is over 200 000.

## 3 Event Selection

E791 has searched for two-, three-, and four-body  $D^0$  decays such as  $D^0 \rightarrow e^+e^-$ ,  $D^0 \rightarrow \phi\mu^+\mu^-$ , and  $D^0 \rightarrow K^-\pi^+\mu^-e^+$ ; and three-body  $D^+$  and  $D_s^+$  decays such as  $D^+ \rightarrow \pi^+\mu^+\mu^-$  and  $D_s^+ \rightarrow K^+\mu^+\mu^-$ . Here and throughout this paper, charge-conjugate modes are included unless otherwise noted. The sensitivity of a search is determined (or normalized) by counting events in a topologically-similar hadronic decay channel such as  $D^+ \rightarrow K^-\pi^+\pi^+$  for

---

<sup>1</sup>The collaboration consists of: CBPF (Brazil), Tel Aviv, CINVESTAV (Mexico), Puebla (Mexico), U. C. Santa Cruz, Cincinnati, Fermilab, Illinois Institute of Technology, Kansas State, Massachusetts, Mississippi, Princeton, South Carolina, Stanford, Tufts, Wisconsin, and Yale.

Table 1: *E791 selection criteria based on tracking and vertexing.*

Selection criteria	Value
$SDZ \equiv$	
$(z_{\text{dec}} - z_{\text{int}})/\sqrt{\sigma_{\text{dec}}^2 + \sigma_{\text{int}}^2}$	$> 20/12/12$ ( $D^+/D_s^+/D^0$ )
$\min z_{\text{dec}} - z_{\text{target edge}} /\sigma_{\text{sec}}$	$> 5$
$z_{\text{dec}} - z_{\text{last target}}$	$< 16$ mm
$\chi_{\text{track}}^2$	$< 5$
$\chi_{\text{vertex}}^2$	$< 6$
$D$ impact parameter (i.p.)	
w/r/t int. vertex	$< 30/40$ $\mu\text{m}$ ( $D^0$ 3-body, 4-body/others)
$\prod_{\text{tracks}} \left( \frac{\text{i.p. w/r/t decay vertex}}{\text{i.p. w/r/t int. vertex}} \right)$	$< 0.01/0.001/0.0005$ (2-body/3-body/4-body)
$p_T$ (transverse to $D$ direction)	$< 0.20/0.25/0.30$ GeV/ $c$ ( $D^+/D_s^+/D^0$ )
$t \equiv m_D \times (z_{\text{dec}} - z_{\text{int}})/p$	$< 5/3/(3 \text{ or } 2.5)$ ps ( $D^+/D_s^+/D^0$ )

which the branching fraction is known. For all searches, the event selection proceeded via a “blind analysis” technique in order to avoid biasing the choice of selection criteria. This technique has three steps: (a) all events having a reconstructed mass within a mass window or “box” around  $m_D$  are removed from the sample; (b) the selection criteria are chosen by optimizing the ratio  $S/\sqrt{B}$ , where  $S$  is the number of signal events from a Monte Carlo simulation that pass all criteria, and  $B$  is the number of events from data that are within a “background box” which is near –but exclusive of– the signal box; (c) the finalized selection criteria are applied to the events within the signal box to see if any candidate events remain. The selection criteria resulting from this procedure are listed in Tables 1 and 2. The most important criterion is that of  $SDZ$ , which is defined as the distance between the interaction vertex and the decay vertex divided by the error in this quantity. Values used for this criterion were 12 for  $D^0$  and  $D_s^+$  decays and 20 for longer-lived  $D^+$  decays.

The mass windows chosen for the various searches depend upon the number of particles in the final state and on whether any of them are electrons. For final states *not* containing electrons, the windows extended  $\pm 35$ ,  $\pm 30$ , or  $\pm 20$  MeV/ $c^2$  around  $m_D$  for  $D^0$ ,  $D^+$ , and  $D_s^+$  decays, respectively. For final states containing one or more electrons, the mass windows were asymmetric,

Table 2: *E791 selection criteria based on particle identification.*

<b>Electron:</b>	EMPROB > 90 (calorimeter response consistent with $e$ )	
<b>Muon:</b>	(1) $p_\mu > 8 \text{ GeV}/c$ (2) $y$ -paddle within $1\sigma$ of track projection is hit (3) $x$ -position as calculated from $y$ -paddle TDC time is within 60 cm of track projection (4) If $y$ -paddle within $1\sigma$ of track projection is <i>not</i> hit, then $x$ -paddle to which track projects is hit	
<b>Kaon:</b>	$P_{\text{Čerenkov}}$ $> 0.10$ $> 0.13$ $> 0.18$	$(D^+ \rightarrow K\pi\pi \text{ norm. for } D_{(s)}^+ \rightarrow \pi\ell\ell)$ $(D^0 \rightarrow K\pi \text{ norm. for } D^0 \rightarrow \ell^+\ell^-,$ $D^0 \rightarrow K\pi\pi\pi \text{ norm. for } D^0 \rightarrow \pi\pi\ell\ell,$ $D^+ \rightarrow K\ell\ell,$ $D^+ \rightarrow K\pi\pi \text{ norm. for } D^+ \rightarrow K\ell\ell)$ $(D_s^+ \rightarrow K\ell\ell,$ $D_s^+ \rightarrow \phi\pi \text{ norm. for } D_s^+ \rightarrow K\ell\ell,$ $D^0 \rightarrow K\pi\ell\ell,$ $D^0 \rightarrow K\pi\pi\pi \text{ norm. for } D^0 \rightarrow K\pi\ell\ell)$

extending 40–70 MeV/ $c^2$  farther below  $m_D$  than above it as the mass distributions had low-energy tails resulting from final-state bremsstrahlung. For search modes containing a  $\rho^0$ ,  $\bar{K}^{*0}$ , or  $\phi$  meson in the final state, it was required that  $|m_{\pi^+\pi^-} - m_\rho| < 150 \text{ MeV}/c^2$ ,  $|m_{K^-\pi^+} - m_{K^*}| < 55 \text{ MeV}/c^2$ , or  $|m_{K^+K^-} - m_\phi| < 10 \text{ MeV}/c^2$ , respectively.

After all selection criteria were applied, no significant excess of events above the estimated background was observed. The experiment thus sets upper limits as follows:

$$UL(D \rightarrow X) = \left( \frac{N_X}{N_{\text{norm}}} \right) \left( \frac{\varepsilon_{\text{norm}}}{\varepsilon_X} \right) \times B_{\text{norm}}, \quad (2)$$

where  $N_X$  is the 90% C.L. upper limit on the mean number of signal events as determined from the number of candidate events observed and the estimated background;  $N_{\text{norm}}$  is the number of events observed (after background subtraction) in a hadronic normalization channel such as  $D^+ \rightarrow K^-\pi^+\pi^+$ ;  $\varepsilon_X$  and  $\varepsilon_{\text{norm}}$  are the overall detection efficiencies for the search channel ( $D \rightarrow X$ ) and

Table 3: *Hadronic decay modes used to normalize the E791 searches for  $D^0 \rightarrow \ell_1^+ \ell_2^-$ ,  $D_{(s)}^+ \rightarrow P \ell_1 \ell_2$ ,  $D^0 \rightarrow V \ell_1^+ \ell_2^-$ , and  $D^0 \rightarrow h_1 h_2 \ell_1 \ell_2$  decays ( $P = \text{pseudoscalar}$ ,  $V = \text{vector}$ ).*

Search mode	Normalization mode	$N_{\text{norm}}$
$D^0 \rightarrow \ell_1^+ \ell_2^-$	$D^0 \rightarrow K^- \pi^+$	$25210 \pm 179$
$D^+ \rightarrow P \ell_1 \ell_2$	$D^+ \rightarrow K^- \pi^+ \pi^+$	$24010 \pm 166$
$D_s^+ \rightarrow P \ell_1 \ell_2$	$D_s^+ \rightarrow \phi \pi^+$	$782 \pm 30$
$D^0 \rightarrow \rho^0 \ell_1^+ \ell_2^-$	$D^0 \rightarrow \pi^+ \pi^- \pi^+ \pi^-$	$2049 \pm 53$
$D^0 \rightarrow \overline{K}^{*0} \ell_1^+ \ell_2^-$	$D^0 \rightarrow \overline{K}^{*0} \pi^+ \pi^-$	$5451 \pm 72$
$D^0 \rightarrow \phi \ell_1^+ \ell_2^-$	$D^0 \rightarrow \phi \pi^+ \pi^-$	$113 \pm 19$
$D^0 \rightarrow \pi \pi \ell_1 \ell_2$	$D^0 \rightarrow \pi^+ \pi^- \pi^+ \pi^-$	$2049 \pm 53$
$D^0 \rightarrow K \pi \ell_1 \ell_2$	$D^0 \rightarrow K^- \pi^+ \pi^- \pi^+$	$11550 \pm 113$
$D^0 \rightarrow K K \ell_1 \ell_2$	$D^0 \rightarrow K^+ K^- \pi^+ \pi^-$	$406 \pm 41$

normalization channel, respectively; and  $B_{\text{norm}}$  is the branching fraction for the normalization channel as taken from the Particle Data Book <sup>4)</sup>. The upper limits  $N_X$  are calculated using the method of Feldman and Cousins <sup>5)</sup> in order to account for estimated background. They are subsequently increased via the prescription of Cousins and Highland <sup>6)</sup> to account for systematic errors.

There were eight hadronic decay channels used for normalization. These channels are listed in Table 3 along with the number of events obtained for each after background subtraction. In general, a dilepton search mode was normalized to a Cabibbo-favored hadronic mode having the same number of tracks in the final state and, whenever possible, the same daughter particles except for the substitution of pions for leptons. For example, the  $D^+ \rightarrow K \ell_1 \ell_2$  searches were normalized to  $D^+ \rightarrow K^- \pi^+ \pi^+$  decays. However, the  $D^0 \rightarrow \rho^0 \ell_1^+ \ell_2^-$  searches were normalized to  $D^0 \rightarrow \pi^+ \pi^- \pi^+ \pi^-$  decays, as there is no published branching fraction for  $D^0 \rightarrow \rho^0 \pi^+ \pi^-$ .

#### 4 Background Estimate

There were two main sources of background in E791: “reflection” background arising from fully-reconstructed hadronic  $D$  decays in which two of the tracks were misidentified as leptons, and “combinatoric” background arising from ac-

Table 4: *Hadronic decay channels contributing reflection background to the E791  $D^0 \rightarrow \ell_1^+ \ell_2^-$ ,  $D_{(s)}^+ \rightarrow P \ell_1 \ell_2$ ,  $D^0 \rightarrow V \ell_1^+ \ell_2^-$ , and  $D^0 \rightarrow h_1 h_2 \ell_1 \ell_2$  samples ( $P = \text{pseudoscalar}$ ,  $V = \text{vector}$ ).*

<b>Cabibbo-favored</b>	<b>Cabibbo-suppressed</b>
$D^0 \rightarrow K^- \pi^+$	$D^0 \rightarrow \pi^+ \pi^-$
$D^+ \rightarrow K^- \pi^+ \pi^+$	$D^+ \rightarrow \pi^- \pi^+ \pi^+$
$D_s^+ \rightarrow \pi^- \pi^+ \pi^+$	$D^+ \rightarrow K^- K^+ \pi^+$
$D_s^+ \rightarrow K^- K^+ \pi^+$	$D_s^+ \rightarrow K^+ \pi^+ \pi^-$
$\Lambda_c^+ \rightarrow p K^- \pi^+$	
$D^0 \rightarrow K^- \pi^+ \pi^- \pi^+$	$D^0 \rightarrow \pi^+ \pi^- \pi^+ \pi^-$
	$D^0 \rightarrow K^+ K^- \pi^+ \pi^-$

cidental combinations of tracks and vertices. Most of the reflection background was eliminated by excluding events with invariant masses (assuming all daughters to be  $\pi$  or  $K$ ) near  $m_D$ ; i.e., it was required that  $|m(h_1 h_2 h_3 h_4) - m_{D^0}| > 35 \text{ MeV}/c^2$ ,  $|m(h_1 h_2 h_3) - m_{D^+}| > 30 \text{ MeV}/c^2$ , and  $|m(h_1 h_2 h_3) - m_{D_s^+}| > 20 \text{ MeV}/c^2$ . These requirements were imposed for all  $h_1 \dots h_4$  final states listed in Table 4, with one exception: those final states having the same number of kaons as that of the search mode were not excluded in this manner, as the acceptance loss for signal events would have been excessive. Instead, background from these modes was estimated as follows.

First, the probability for a pair of pions to be misidentified as  $\mu\mu$ ,  $\mu e$ , or  $ee$  was estimated from data. This probability was then multiplied by the number of events observed in the hadronic channel for which the reflection cut could not be applied. A factor was included to account for the fraction of these events that would reflect into the signal mass window if two daughter pions were misidentified as leptons. For example, the reflection background in the  $D^+ \rightarrow \pi^+ \mu^+ \mu^-$  sample arising from  $D^+ \rightarrow \pi^- \pi^+ \pi^+$  decays is calculated as  $P_{\pi\pi \rightarrow \mu\mu} \times N_{\pi^- \pi^+ \pi^+} \times f \times J_c$ , where  $f$  is the fraction of  $D^+ \rightarrow \pi^- \pi^+ \pi^+$  decays that would reflect into the  $D^+$  mass window if two daughter pions were misidentified as muons (75% in this example). The factor  $J_c$  accounts for the different ways a hadronic mode can be misidentified as a dilepton mode; e.g., there are two ways that  $D^+ \rightarrow \pi^- \pi^+ \pi^+$  can be misidentified as  $D^+ \rightarrow \pi^+ \mu^+ \mu^-$ .

The misidentification probabilities for three-body decays were obtained from the final  $D^+ \rightarrow K^- \ell_1^+ \ell_2^+$  samples, and those for four-body decays from the final  $D^0 \rightarrow K^- \pi^+ \ell_1^- \ell_2^+$  samples, where all candidates observed (after subtracting combinatoric background estimated from mass sidebands) were assumed to originate from  $D^+ \rightarrow K^- \pi^+ \pi^+$  and  $D^0 \rightarrow K^- \pi^+ \pi^- \pi^+$  decays, respectively. For example, there were 13, 5.2, and 6 events passing all selection criteria for the  $K^- \mu^+ \mu^+$ ,  $K^- \mu^+ e^+$ , and  $K^- e^+ e^+$  samples, respectively, and 17 730 events (after background subtraction) in the  $D^+ \rightarrow K^- \pi^+ \pi^+$  sample. Thus, the misidentification probabilities for three-body decays were  $P_{\mu\mu} = (7.3 \pm 2.0) \times 10^{-4}$ ,  $P_{\mu e} = (2.9 \pm 1.3) \times 10^{-4}$ , and  $P_{ee} = (3.4 \pm 1.4) \times 10^{-4}$ . The reflection backgrounds for the  $D^+ \rightarrow K^- \ell_1^+ \ell_2^+$  and  $D^0 \rightarrow K^- \pi^+ \ell_1^- \ell_2^+$  modes themselves were taken to be zero as there was no independent estimate of the misidentification rates. This results in conservative upper limits. Unfortunately, there were too many events observed for the  $D^+ \rightarrow K^- \ell_1^+ \ell_2^+$  modes (after accounting for combinatoric background – see below) to set meaningful upper limits.

After the mass reflection cuts, combinatoric background was estimated by averaging the number of events in the mass sidebands both above and below the  $D$  signal mass window and scaling this number by the size of the signal mass window relative to that of the mass sidebands. If there were no events in the higher mass sideband, it was assumed that there were no combinatoric background events in the signal box. This assumption avoids overestimating background due to statistical fluctuations. Because it tends to underestimate background, it results in a conservative upper limit.

There were also small backgrounds to the  $D^0 \rightarrow K^- \pi^+ \ell^+ \ell^-$ ,  $D^0 \rightarrow K^+ K^- \ell^+ \ell^-$ ,  $D^0 \rightarrow \bar{K}^{*0} \ell^+ \ell^-$ , and  $D^0 \rightarrow \phi \ell^+ \ell^-$  samples arising from  $D^0 \rightarrow K^- \pi^+ \rho^0$ ,  $D^0 \rightarrow K^+ K^- \rho^0$ ,  $D^0 \rightarrow \bar{K}^{*0} \rho^0$ , and  $D^0 \rightarrow \phi \rho^0$  decays, respectively, where  $\rho^0 \rightarrow \ell^+ \ell^-$ . These backgrounds were estimated using the branching fractions for  $D^0 \rightarrow h_1 h_2 \rho^0$ ,  $D^0 \rightarrow V \rho^0$ , and  $\rho^0 \rightarrow \ell^+ \ell^-$  from the Particle Data Book <sup>4</sup>).

## 5 Upper Limits

The final event samples after all selection criteria were applied and signal boxes “opened” are shown in Figs. 2-3. The number of background events estimated, the number of candidate events observed, the overall systematic error, and the resultant 90% C.L. upper limits are listed in Tables 5 and 6. The systematic



errors arise mainly from four sources: errors resulting from the fits to the normalization channels, statistical errors on the number of Monte Carlo events generated and accepted (used to calculate acceptance), uncertainties in the amounts of reflection and combinatoric background, and uncertainties in the relative detection efficiencies between the search modes and their normalization channels. The upper limits on the branching fractions are compared to (previous) limits from the Particle Data Book <sup>4)</sup> in Fig. 4. Of the 51 decay modes listed, all but six have upper limits more stringent than previously published results. For 26 of these modes, the E791 limits are the first such limits reported.

## 6 Other Experiments

There are five published limits that remain superior to those obtained by E791, and one published limit that is equivalent. These were obtained by the CLEO experiment <sup>7)</sup> ( $D^0 \rightarrow \rho^0 e^+ e^-$ ,  $\rho^0 \mu^\pm e^\mp$ ,  $\phi e^+ e^-$ ,  $\phi \mu^\pm e^\mp$ ), by the BEATRICE experiment <sup>8)</sup> ( $D^0 \rightarrow \mu^+ \mu^-$ ), and by FNAL E687 <sup>9)</sup> ( $D^+ \rightarrow K^+ e^+ e^-$ ). This last experiment used a photon beam of mean energy  $\sim 220$  GeV to photoproduce charm, and a silicon strip vertex detector (like E791) to reconstruct  $D$  decay vertices. The experiment ran concurrently with E791 and obtained an upper limit for  $B(D^+ \rightarrow K^+ e^+ e^-)$  identical to that from E791.

Another hadroproduction experiment, FNAL E771 <sup>10)</sup>, also ran concurrently with E791 but used an 800 GeV/c proton beam. This experiment obtained an upper limit for  $B(D^0 \rightarrow \mu^+ \mu^-)$  remarkably close to that obtained by BEATRICE. In fact, the 90% C.L. upper limits from BEATRICE, E771, and E791 are within about 25% of each other:  $B(D^0 \rightarrow \mu^+ \mu^-) < 4.1, 4.2,$  and  $5.2 \times 10^{-6}$ , respectively. Assuming these results uncorrelated, we combine them to obtain  $B(D^0 \rightarrow \mu^+ \mu^-) < 1.5 \times 10^{-6}$  at 90% C.L. This limit is still many orders of magnitude larger than the Standard Model expectation <sup>11)</sup> (dominated by long-distance effects) of  $\sim 10^{-15}$ .

For the future, we expect greater sensitivity than that of the above experiments from FNAL E831 (FOCUS) <sup>12)</sup>, a photoproduction experiment that is an upgraded version of E687. The E831 detector employed more muon counters than did E791 and also used a finer-grained electromagnetic calorimeter. The experiment took data in 1996–97, recording a charm sample approximately four times larger than that of E791. The analysis of this data set is underway.

## 7 Summary

In summary, E791 has completed an extensive search for flavor-changing neutral-current, lepton-flavor-violating, and lepton-number-violating processes and sees no evidence for these decays. The experiment has set upper limits on 51 different decay modes; all limits but six are improvements over previously published results. Many of these limits are at the  $10^{-5}$  to  $10^{-6}$  level and can constrain various extensions<sup>13)</sup> to the Standard Model. We anticipate even more stringent limits (or possibly signals) from E831, which has a “cleaner” data sample due to the photoproduction process, superior muon and electron identification, and approximately four times as many reconstructed charm decays.

## References

1. E. M. Aitala *et al.*, Phys. Rev. Lett. **76**, 364 (1996); Phys. Lett. **B462**, 401 (1999).
2. E. M. Aitala *et al.*, FERMILAB-Pub-00/280-E (2000), hep-ex/0011077 (submitted to Phys. Rev. Lett.).
3. E. M. Aitala *et al.*, Eur. Phys. J. direct **C4**, 1 (1999).  
See also: E. M. Aitala *et al.*, Phys. Lett. **B371**, 157 (1996); Phys. Rev. **D57**, 13 (1998).
4. D. E. Groom *et al.* (Particle Data Group), Eur. Phys. J. **C15**, 1 (2000);  
C. Caso *et al.* (Particle Data Group), Eur. Phys. J. **C3**, 1 (1998).
5. G. J. Feldman and R. D. Cousins, Phys. Rev. **D57**, 3873 (1998).
6. R. D. Cousins and V. L. Highland, Nucl. Instrum. Meth. **A320**, 331 (1992).
7. A. Freyberger *et al.*, Phys. Rev. Lett. **76**, 3065 (1996); Phys. Rev. Lett. **77**, 2147 (1996).
8. M. Adamovich *et al.*, Phys. Lett. **B408**, 469 (1997).
9. P. L. Frabetti *et al.*, Phys. Lett. **B398**, 239 (1997).
10. T. Alexopoulos *et al.*, Phys. Rev. Lett. **77**, 2380 (1996).
11. S. Pakvasa, UH-511-871-97 (1997), hep-ph/9705397.

12. P. D. Sheldon, Charm Mixing and Rare Decays, in: Heavy Flavors 8, Proc. of the 8th Int. Symp. on Heavy Flavour Physics, Southampton, UK, 25-29 July 1999 (The Journal of High Energy Physics Conf. Proceedings, eds. P. Dauncey and C. Sachrajda, <http://jhep.sissa.it>).  
See also: J. M. Link *et al.*, Phys. Lett. **B485**, 62 (2000); Phys. Lett. **B491**, 232 (2000).
13. See for example: G. López Castro, R. Martínez, and J. H. Muñoz, Phys. Rev. **D58**, 033003 (1998).

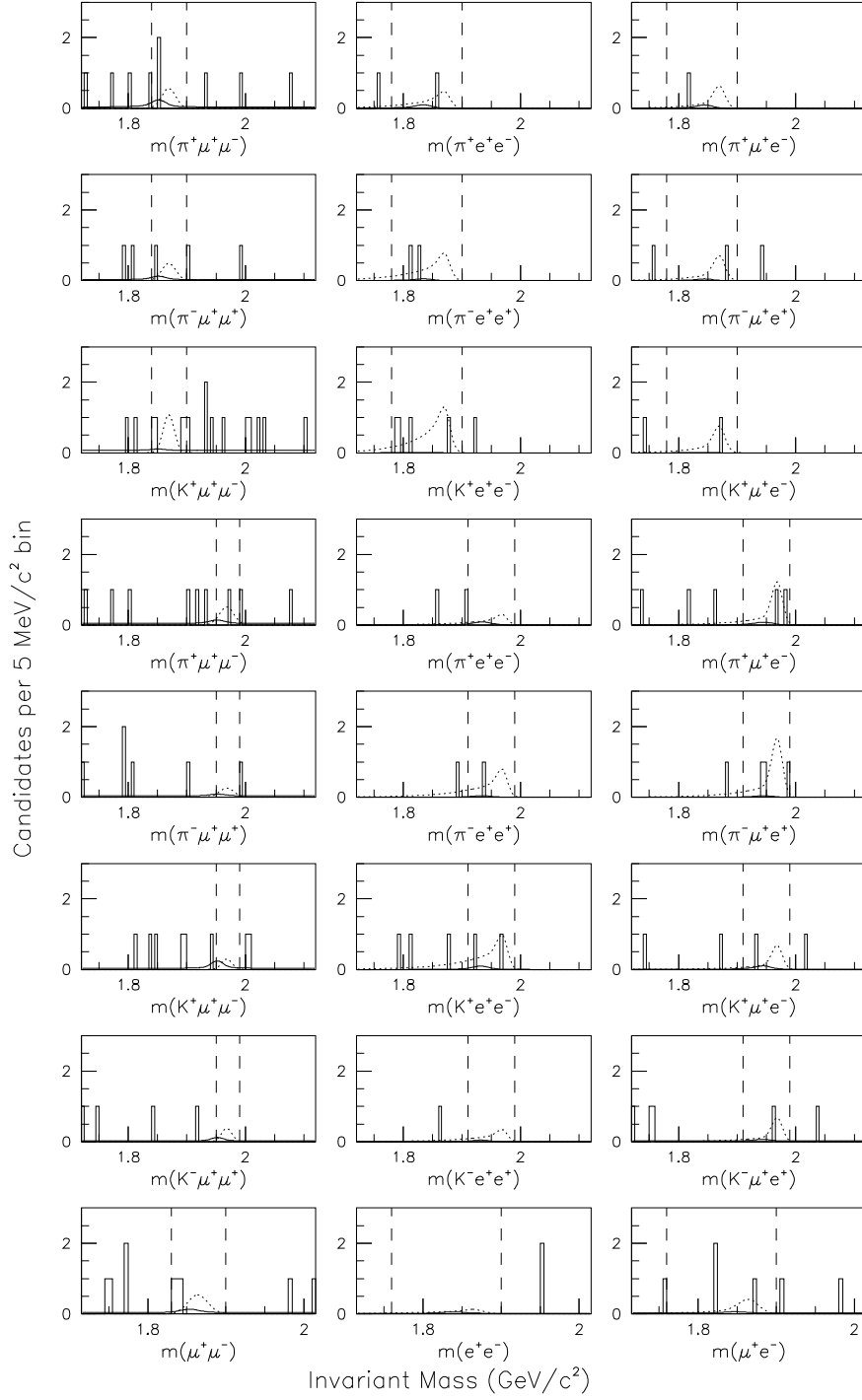


Figure 2:  $D^+ \rightarrow P \ell_1 \ell_2$  (rows 1–3),  $D_s^+ \rightarrow P \ell_1 \ell_2$  (rows 4–7), and  $D^0 \rightarrow \ell_1^+ \ell_2^-$  (row 8) event samples. The solid curves represent estimated background; the dotted curves represent signal shape for an event yield equal to the 90% C.L. upper limit; the dashed vertical lines denote the signal mass windows.

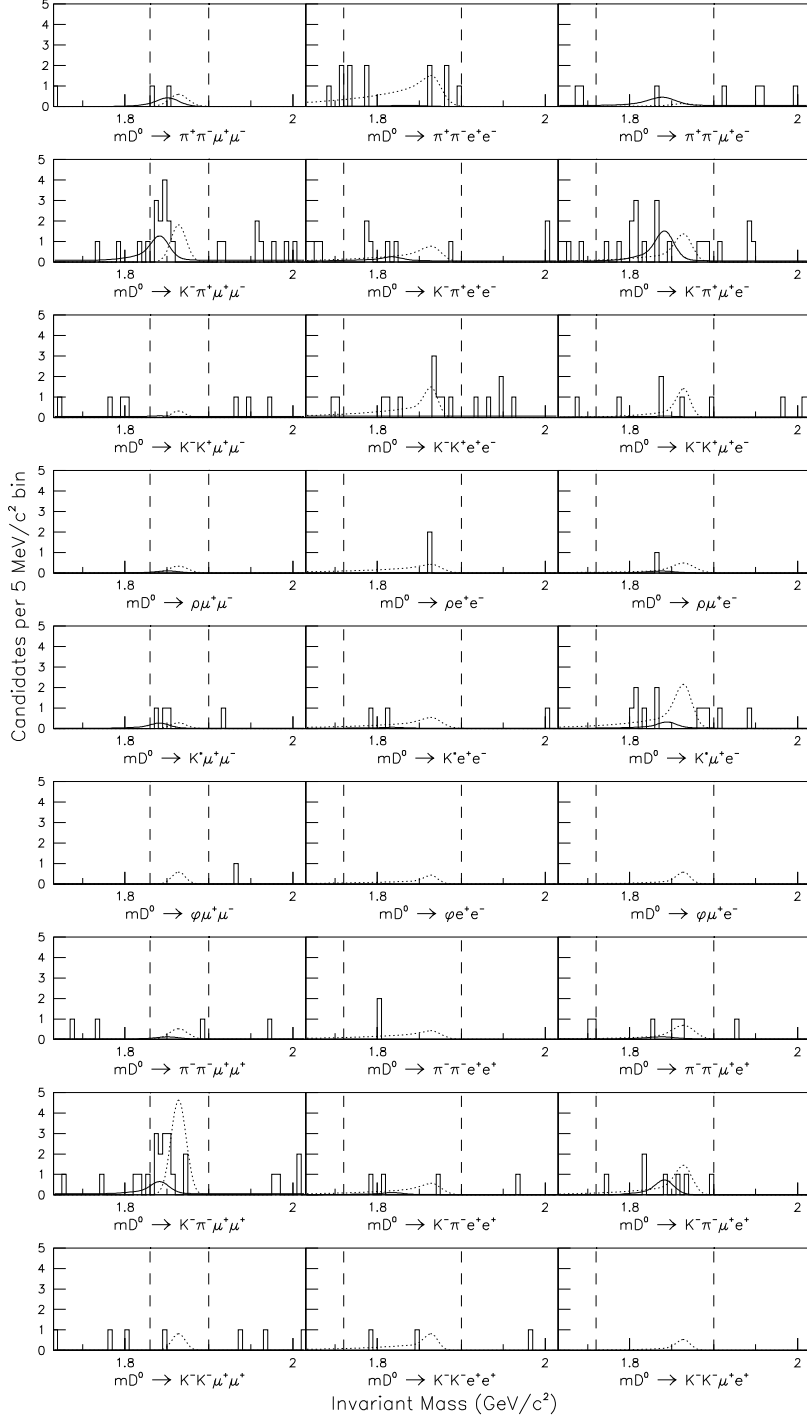


Figure 3: Final  $D^0 \rightarrow V l_1^+ l_2^-$  and  $D^0 \rightarrow h_1 h_2 l_1 l_2$  event samples for nonresonant modes (rows 1–3), resonant modes (rows 4–6), and same-signed dilepton modes (rows 7–9). The solid curves represent estimated background; the dotted curves represent signal shape for an event yield equal to the 90% C.L. upper limit; the dashed vertical lines denote the signal mass windows.

Table 5: The number of background events estimated, the number of candidate events observed, the overall systematic error, and the 90% C.L. upper limits on  $N_X$  and the branching fraction for  $D^0 \rightarrow \ell_1^+ \ell_2^-$  and  $D_{(s)}^+ \rightarrow P \ell_1 \ell_2$  decays.

Mode	Est. background			$N_{\text{obs}}$	System. Err. (%)	$N_X$	BR $\times 10^{-5}$
	$N_{\text{comb}}$	$N_{\text{misID}}$	$N_{\text{tot}}$				
$D^0 \rightarrow \mu^+ \mu^-$	1.83	0.63	2.46	2	6	3.51	0.52
$D^0 \rightarrow e^+ e^-$	1.75	0.29	2.04	0	9	1.26	0.62
$D^0 \rightarrow \mu^\pm e^\mp$	2.63	0.25	2.88	2	7	3.09	0.81
$D^+ \rightarrow \pi^+ \mu^+ \mu^-$	1.20	1.47	2.67	2	10	3.35	1.5
$D^+ \rightarrow \pi^+ e^+ e^-$	0.00	0.90	0.90	1	12	3.53	5.2
$D^+ \rightarrow \pi^+ \mu^\pm e^\mp$	0.00	0.78	0.78	1	11	3.64	3.4
$D^+ \rightarrow \pi^- \mu^+ \mu^+$	0.80	0.73	1.53	1	9	2.92	1.7
$D^+ \rightarrow \pi^- e^+ e^+$	0.00	0.45	0.45	2	12	5.60	9.6
$D^+ \rightarrow \pi^- \mu^+ e^+$	0.00	0.39	0.39	1	11	4.05	5.0
$D^+ \rightarrow K^+ \mu^+ \mu^-$	2.20	0.20	2.40	3	8	5.07	4.4
$D^+ \rightarrow K^+ e^+ e^-$	0.00	0.09	0.09	4	11	8.72	20
$D^+ \rightarrow K^+ \mu^\pm e^\mp$	0.00	0.08	0.08	1	9	4.34	6.8
$D_s^+ \rightarrow K^+ \mu^+ \mu^-$	0.67	1.33	2.00	0	27	1.32	14
$D_s^+ \rightarrow K^+ e^+ e^-$	0.00	0.85	0.85	2	29	5.77	160
$D_s^+ \rightarrow K^+ \mu^\pm e^\mp$	0.40	0.70	1.10	1	27	3.57	63
$D_s^+ \rightarrow K^- \mu^+ \mu^+$	0.40	0.64	1.04	0	26	1.68	18
$D_s^+ \rightarrow K^- e^+ e^+$	0.00	0.39	0.39	0	28	2.22	63
$D_s^+ \rightarrow K^- \mu^+ e^+$	0.80	0.35	1.15	1	27	3.53	68
$D_s^+ \rightarrow \pi^+ \mu^+ \mu^-$	0.93	0.72	1.65	1	27	3.02	14
$D_s^+ \rightarrow \pi^+ e^+ e^-$	0.00	0.83	0.83	0	29	1.85	27
$D_s^+ \rightarrow \pi^+ \mu^\pm e^\mp$	0.00	0.72	0.72	2	30	6.01	61
$D_s^+ \rightarrow \pi^- \mu^+ \mu^+$	0.80	0.36	1.16	0	27	1.60	8.2
$D_s^+ \rightarrow \pi^- e^+ e^+$	0.00	0.42	0.42	1	29	4.44	69
$D_s^+ \rightarrow \pi^- \mu^+ e^+$	0.00	0.36	0.36	3	28	8.21	73

Table 6: *The number of background events estimated, the number of candidate events observed, the overall systematic error, and the 90% C.L. upper limits on  $N_X$  and the branching fraction for  $D^0 \rightarrow V\ell_1^+\ell_2^-$  and  $D^0 \rightarrow h_1h_2\ell_1\ell_2$  decays. The total background estimate ( $N_{tot}$ ) includes small contributions from  $D^0 \rightarrow K^-\pi^+\rho^0$ ,  $D^0 \rightarrow K^+K^-\rho^0$ ,  $D^0 \rightarrow \bar{K}^{*0}\rho^0$ , and  $D^0 \rightarrow \phi\rho^0$ , where  $\rho^0 \rightarrow \ell^+\ell^-$ .*

Mode	Est. background			$N_{\text{obs}}$	System. Err. (%)	$N_X$	BR $\times 10^{-5}$
	$N_{\text{comb}}$	$N_{\text{misID}}$	$N_{\text{tot}}$				
$\pi^+\pi^-\mu^+\mu^-$	0.00	3.16	3.16	2	11	2.96	3.0
$\pi^+\pi^-e^+e^-$	0.00	0.73	0.73	9	12	15.2	37
$\pi^+\pi^-\mu^\pm e^\mp$	5.25	3.46	8.71	1	15	1.06	1.5
$K^-\pi^+\mu^+\mu^-$	3.65	0	4.10	12	11	15.4	36
$K^-\pi^+e^+e^-$	3.50	0	3.94	6	15	7.53	39
$K^-\pi^+\mu^\pm e^\mp$	5.25	0	5.25	15	12	17.3	55
$K^+K^-\mu^+\mu^-$	2.13	0.17	2.37	0	17	1.22	3.3
$K^+K^-e^+e^-$	6.13	0.04	6.23	9	18	9.61	32
$K^+K^-\mu^\pm e^\mp$	3.50	0.17	3.67	5	17	6.61	18
$\rho^0\mu^+\mu^-$	0.00	0.75	0.75	0	10	1.80	2.2
$\rho^0e^+e^-$	0.00	0.18	0.18	1	12	4.28	12
$\rho^0\mu^\pm e^\mp$	0.00	0.82	0.82	1	11	3.60	6.6
$\bar{K}^{*0}\mu^+\mu^-$	0.30	1.87	2.43	3	24	5.40	2.4
$\bar{K}^{*0}e^+e^-$	0.88	0.49	1.62	2	25	4.68	4.7
$\bar{K}^{*0}\mu^\pm e^\mp$	1.75	2.30	4.05	9	24	12.8	8.3
$\phi\mu^+\mu^-$	0.30	0.04	0.35	0	33	2.33	3.1
$\phi e^+e^-$	0.00	0.01	0.01	0	33	2.75	5.9
$\phi\mu^\pm e^\mp$	0.00	0.05	0.05	0	33	2.71	4.7
$\pi^-\pi^-\mu^+\mu^+$	0.91	0.79	1.70	1	9	2.78	2.9
$\pi^-\pi^-e^+e^+$	0.00	0.18	0.18	1	11	4.26	11
$\pi^-\pi^-\mu^+e^+$	2.63	0.86	3.49	4	10	5.18	7.9
$K^-\pi^-\mu^+\mu^+$	2.74	3.96	6.69	14	9	15.7	39
$K^-\pi^-e^+e^+$	0.88	1.04	1.91	2	16	4.14	21
$K^-\pi^-\mu^+e^+$	0.00	4.88	4.88	7	11	7.81	22
$K^-K^-\mu^+\mu^+$	1.22	0.00	1.22	1	17	3.27	9.4
$K^-K^-e^+e^+$	0.88	0.00	0.88	2	17	5.28	15
$K^-K^-\mu^+e^+$	0.00	0.00	0.00	0	17	2.52	5.7

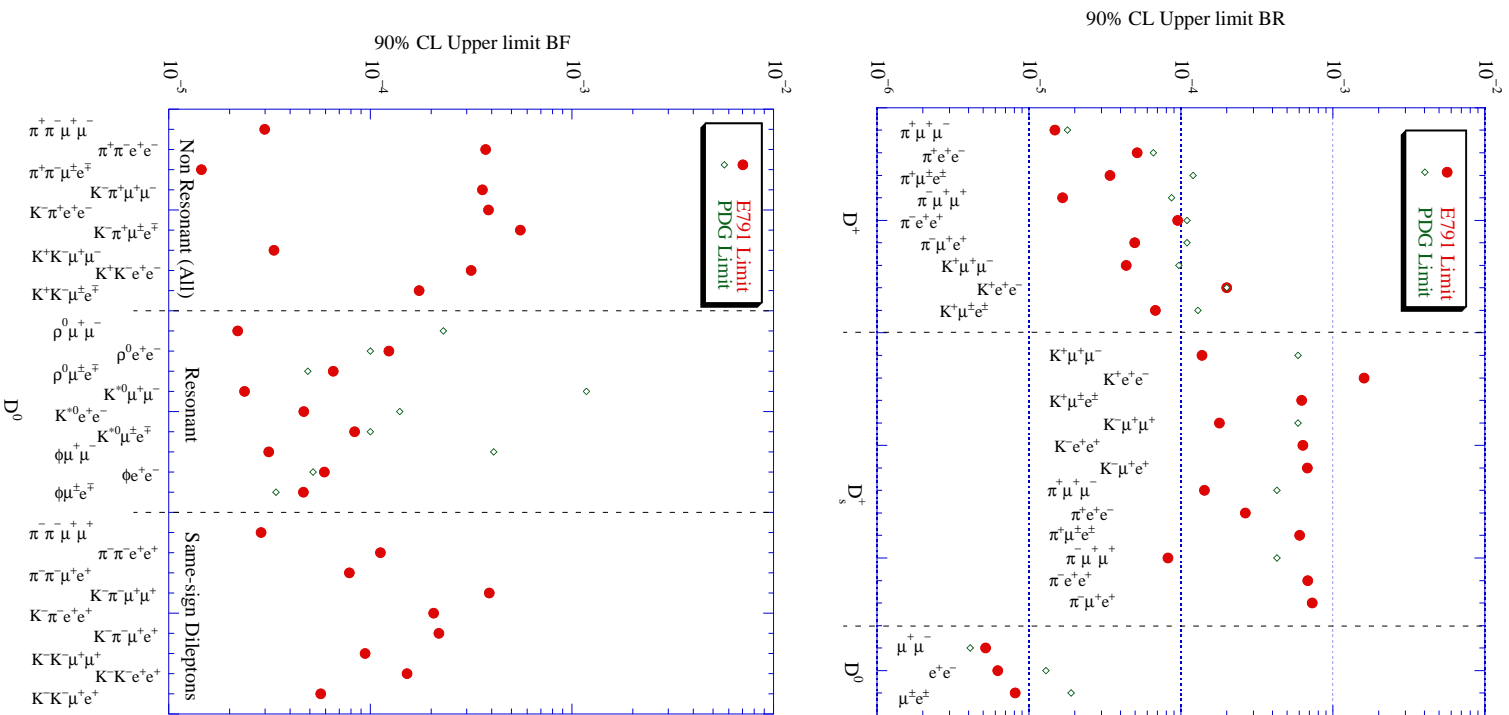


Figure 4: Upper limits for  $D^0 \rightarrow \ell_1^+ \ell_2^-$  and  $D_s^+ \rightarrow P \ell_1 \ell_2$  decays (top), and  $D^0 \rightarrow V \ell_1^+ \ell_2^-$  and  $D^0 \rightarrow h_1 h_2 \ell_1 \ell_2$  decays (bottom). The circles are E791 limits 1, 2) and the diamonds are (previous) limits from the Particle Data Book 4).